symmetry

Article

Heat Transfer in an Inclined Rectangular Cavity Filled with Hybrid Nanofluid Attached to a Vertical Heated Wall Integrated with PCM: An Experimental Study

Muqdad Al-Maliki [1], Khaled Al-Farhany [1,*] and Ioannis E. Sarris [2,*]

[1] Department of Mechanical Engineering, University of Al-Qadisiyah, Al-Qadisiyah 58001, Iraq
[2] Department of Mechanical Engineering, University of West Attica, 250 Thivon & P. Ralli Str., Egaleo, 12244 Athens, Greece
* Correspondence: khaled.alfarhany@qu.edu.iq (K.A.-F.); sarris@uniwa.gr (I.E.S.)

Abstract: In this paper, natural convective heat transfer in a rectangular cavity filled with (50% CuO-50% Al_2O_3)/water hybrid nanofluids connected to a wall containing a phase change material (PCM) has been experimentally investigated. The vertical walls were heated at varying temperatures while the horizontal walls were kept adiabatic. The considered parameters were the concentration of hybrid nanomaterial (Φ = 0.03, 0.05), the cavity inclination angle (θ = 0°, 30°, 45°), and the temperature difference between the hot and cold sides (ΔT = 10, 15, 20 °C). The results have been validated and agree well with previously published papers. Furthermore, the main results stated that when the nanomaterial concentration increased, the heat transfer rate by free convection also increased. By increasing the natural convection flows via high temperature, symmetrical vortexes may appear near the heated wall. It also found that the PCM can potentially reduce the temperature of the hot side by up to 22% due to its high absorbability and heat storage. Furthermore, the inclusion of hybrid nanofluids in addition to the PCM enhanced its efficiency in heat storage and, therefore, its capacity to cool the hot side. Moreover, the influence of the inclination cavity enhanced the heat transfer, where θ = 30° was the optimal angle in terms of thermal conductivity.

Keywords: hybrid nanofluid; inclined cavity; natural convection; PCM; rectangular cavity

Citation: Al-Maliki, M.; Al-Farhany, K.; Sarris, I.E. Heat Transfer in an Inclined Rectangular Cavity Filled with Hybrid Nanofluid Attached to a Vertical Heated Wall Integrated with PCM: An Experimental Study. *Symmetry* **2022**, *14*, 2181. https://doi.org/10.3390/sym14102181

Academic Editor: Vasilis K. Oikonomou

Received: 20 September 2022
Accepted: 13 October 2022
Published: 17 October 2022

1. Introduction

Many applications, including solar energy and electronic cooling, rely heavily on convective heat transfer characteristics. For that reason, many experimental and theoretical investigations have been conducted to study natural heat transfer using active and passive techniques. Some authors have added nanoparticles to a base fluid to enhance the working fluid's thermal conductivity [1–5]. Other researchers have studied hybrid nanofluids and their effects on improving heat transfer [6–12]. Some researchers have also found that using a phase change material (PCM) can help manage heat transfer, which led authors to discover its importance in thermal storage [13–26].

Shili et al. [27] experimentally and numerically examined the impact of liquid selection on a PCM. Water and SilOil were used in the proximity of a phase transition material (synthetic paraffin). The considered cavity, a rectangular container, was filled with phase change material (PCM) and heated from the left side while the other walls were kept isolated. The novelty of the study is that it separated the hot plate from the PCM by a layer of liquid, water, or SilOil. The findings indicated that restricting the PCM in the liquid increases thermal conductivity at the hot plate, improves heat transmission, and protects the PCM from overheating. In addition, when water surrounds the PCM, the copper sheet temperature decreases by approximately 20%. Kean et al. [28] numerically studied the effect on free convection of a PCM combined with nanomaterials in a square cavity. The authors considered two cases: the first assumed that the vertical walls were the hot and cold walls and isolated the horizontal walls; the second considered the horizontal walls as hot and cold walls and isolated the vertical walls. The authors considered different types of nanoparticles, such as alumina, copper oxide, and zinc oxide in various volume fractions (Φ = 0, 0.02, and 0.05). The findings revealed that adding nanoparticles with a low volume fraction can enhance the performance of the PCM. Furthermore, the wax melted in the first case faster than in the second case.

Sivashankar et al. [29] investigated heat transfer in concentrated photovoltaic (CPV) cells utilizing a phase change material (PCM) and graphene nanoplatelets (GNP). The efficiency of a CPV cell with a pure PCM was investigated and compared to the efficiency in the case of using a nano-augmented PCM (n-PCM) with a range of concentrations (0.1%-0.5%). The results stated that the efficiency of the CPV was much higher when using the nano-augmented PCM than the pure PCM. Ebadi et al. [30] numerically studied the effect of a bio-based nanoPCM on heat transfer in a perpendicular cylindrical thermal energy storage (C-TES) system. The variables which were considered were a Ra number ($10^6 \leq Ra \leq 10^8$) and the solid volume proportion of the hybrid nanofluid ($0 \leq \varphi \leq 0.05$). The results showed that the value of Nu_{avg} increased at the early stage of the melting and then dropped sharply with time. Furthermore, as the nanoparticle volume fraction increased, the stored energy decreased. It is worth mentioning that the results stated that the importance of solidification and melting had the same effect on performance. Abdelrazik et al. [31] numerically discussed the impact of a nano-PCM on thermal and electrical performance. The results stated that using the PCM increased the efficiency of the panel's cooling, which leads to higher electrical efficiency. Nada et al. [32] numerically examined the temperature management and efficiency of PV-building integrated systems using phase change materials and Al_2O_3 nanoparticles. Two separate PV-PCM modules were produced using pure PCM and PCM with added nanoparticles. The characteristics used were solar radiation intensity, wind speed, and PV voltage. The results showed that adding Al_2O_3 nanoparticles to the PCM improved the integrated modules' heat efficiency and temperature management. Integrating the PV units with pure PCM and PCM augmented by nanoparticles lowered the temperature of the modules by 8.1 and 10.6 °C, while the efficiency rose by 5.7 and 13.2%, respectively. Chavan et al. [33] performed a numerical inquiry of natural convection of the melting process in a rectangular enclosure. A compound phase change material (paraffin wax 98%) was utilized as the base material, with the addition of copper nanoparticles (2%). One side of the container was heated, the other was isothermal, and the different sides were thermally insulated. An enclosed domain with two distinct directions, enclosures that were both deep and shallow, was assumed for the thermal storage model. The results showed that the shallow enclosure showed a quicker rate of charging and discharging than the large enclosure (up to 10% less).

From the previous literature, it can be noticed that there is a lack of experimental work; for that reason, this paper introduces a novel geometry, which is an application of solar energy, to investigate the free convection of hybrid nanofluid flow in a uniform cavity with a PCM material. A wide range of volume concentrations, temperature gradients, and inclination angles were considered in order to understand their effect on flow streams and heat transfer.

2. Experimental Work

2.1. Test Rig

This section describes the main parts of the experimental setup. Figure 1 shows the schematic diagram of the experimental design, while the experimental setup apparatus can be seen in Figure 2. A cavity containing a hybrid nanofluid was combined with another cavity with a phase change material. In this portion, the heating system (which consisted of a heater, a controller, and a DC power supply), the cooling unit (constant temperature water bath), and the measuring system (thermal camera, data logger tool) are installed.

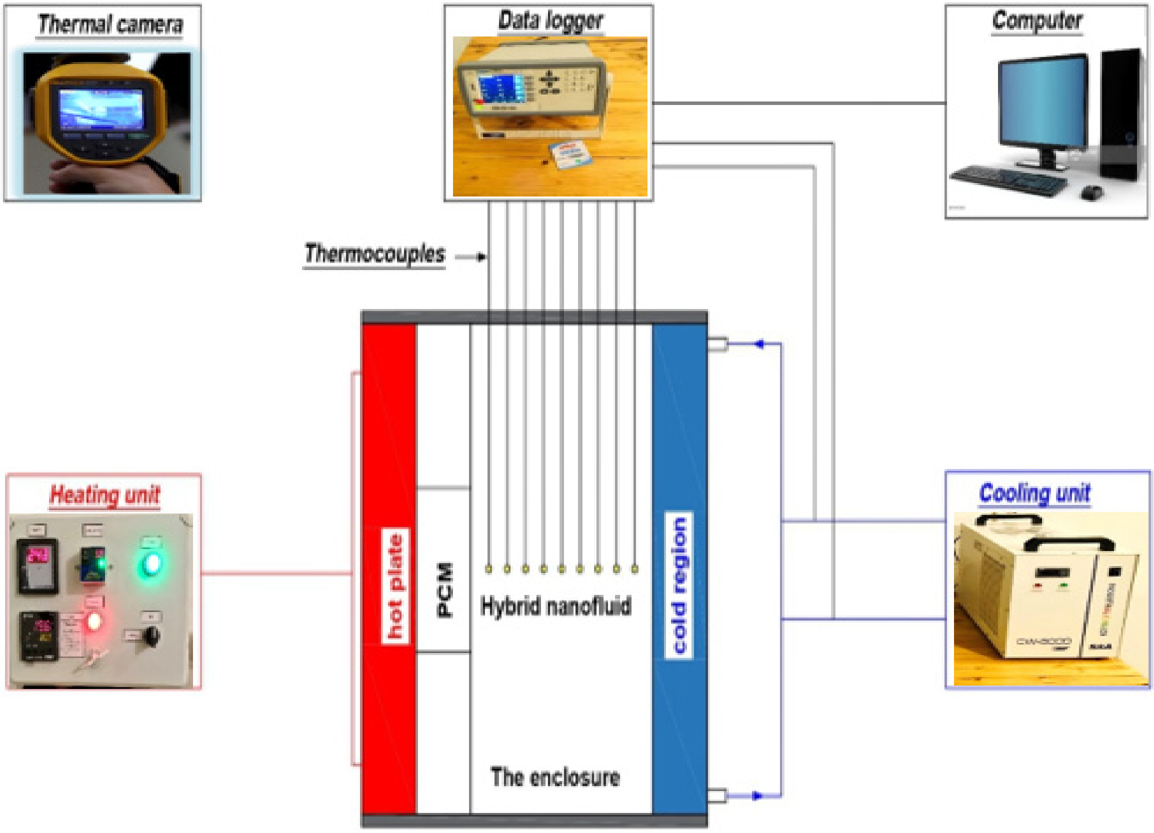

Figure 1. Schematic diagram of the experimental setup.

Figure 2. Experimental setup apparatus: (**1**) sensitive balance, (**2**) mechanical stirrer, (**3**) ultrasonic wave apparatus, (**4**) Fluke Ti300 thermal imaging camera, (**5**) datalogger, PC, and test section.

2.2. Test of the Physical Problem

Figure 3 depicts the test section, which consisted of two rectangular cavities. The left, connected to the hot wall, consisted of an aluminum plate heated by an electric temperature control heater. The left cavity was 20 cm high, 3 cm wide, and 20 cm deep, and was divided into three horizontal grooves filled with PCM. The right side of the second cavity was connected to the cold wall. It was 20 cm high, 10 cm wide, and 20 cm deep, and was meant to operate as a thermal exchanger. It was constructed of an aluminum plate and adjusted the temperature by running water through it. It was filled with a hybrid nanofluid; Table 1 shows the physical properties of the fluid and nanoparticles [34], while Table 2 shows the PCM properties [35]. Three thermocouples were inserted in each of the two walls to detect temperatures, and 35 thermocouples were installed in the center of the cavity to assess temperature dispersion throughout the case.

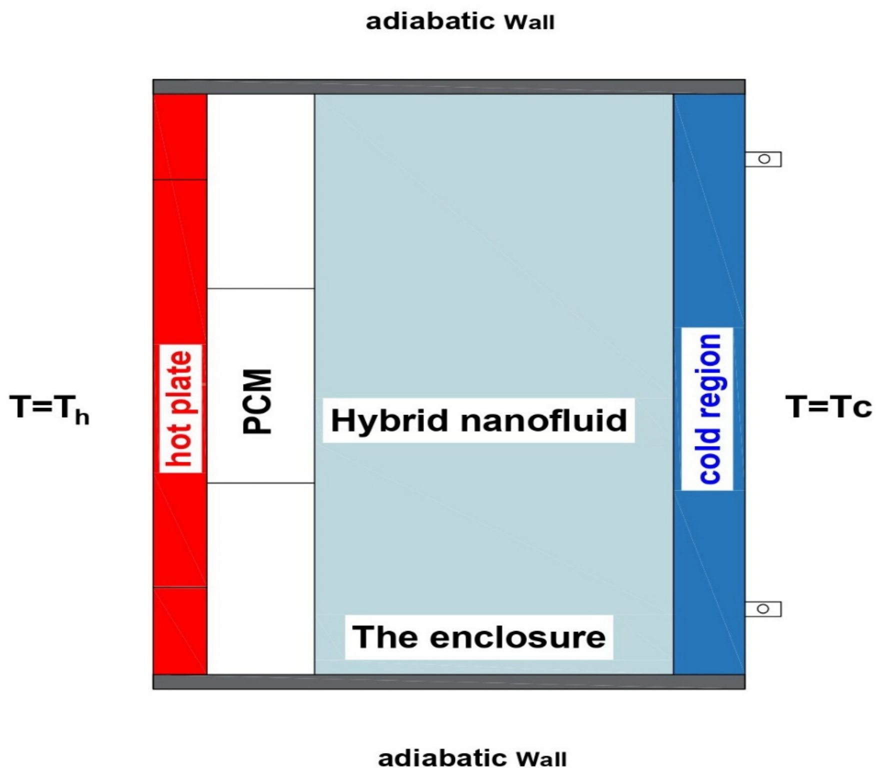

Figure 3. Schematic description of the physical model.

Table 1. Thermophysical properties of some nanoparticles and water [34].

Property	Pure Water	Al_2O_3	CuO
ρ (kg/m^3)	997.1	3970	6500
Cp (J/kg·K)	4179	765	540
k (W/m·K)	0.613	40	18.0
ν [m^2/s]	0.891×10^{-6}	—-	—-
β [1/T] (1/K)	2.1×10^{-4}	8.5×10^{-6}	0.85×10^{-5}
α (m^2/s)	1.47×10^{-7}	13.17×10^{-6}	51.28×10^{-7}

Table 2. Thermophysical properties of PCM [35].

T-Solidus	38 °C
T-liquidus	43 °C
Latent heat of melting	174 kJ/kg
Density	800 kg/m^3 (solid) 760 kg/m^3 (liquid)
Thermal expansion coefficient	0.00081/°k
Specific heat capacity	2 kJ/kg·K
Thermal conductivity	0.2 W/m·K

3. The Effective Thermophysical Properties of Hybrid Nanofluid

The relations that describe the effective physical properties of nanofluid in this study, determined according to the following equations [36,37], are:

The density of hybrid nanofluid ρ_{hnf} is:

$$\varphi_{hnf} = \varphi_{Cuo} + \varphi_{Al2o3} \tag{1}$$

$$\rho_{hnf} = \varphi_{Cuo} \cdot \rho_{Cuo} + \varphi_{Al2o3} \cdot \rho_{Al2o3} + \left(1 - \varphi_{hnf}\right) \cdot \rho_{bf} \tag{2}$$

$$\rho_{hnf} \cdot Cp_{hnf} = \varphi_{Cuo} \cdot \rho_{Cuo} \cdot Cp_{Cuo} + \varphi_{Al2O3} \cdot \rho_{Al2O3} \cdot Cp_{Al2O3} + \left(1 - \varphi_{hnf}\right) \cdot \rho_{bf} \cdot Cp_{bf} \tag{3}$$

$$(\rho\beta)_{hnf} = \varphi_{Cuo} \cdot \rho_{Cuo} \cdot \beta_{Cuo} + \varphi_{Al2O3} \cdot \rho_{Al2O3} \cdot \beta_{Al2O3} + \left(1 - \varphi_{hnf}\right) \cdot \rho_{bf} \cdot \beta_{bf} \tag{4}$$

The dynamic viscosity ratio of hybrid nanofluid is estimated using the Brinkman and Maxwell model, given by [38] as follows:

$$\frac{\mu_{hnf}}{\mu_{bf}} = \frac{1}{(1 - (\varphi_{Cuo} + \varphi_{Al2O3})^{2.5}} \tag{5}$$

The thermal conductivity is found by using the Maxwell correlation [38]:

$$\frac{k_{hnf}}{k_{bf}} = \frac{\left(\frac{(\varphi_{Cuo} \cdot k_{cuo} + \varphi_{Al2O3} \cdot k_{Al2o3})}{\varnothing_{hnf}} + 2kbf + 2(\varphi_{Cuo} \cdot k_{cuo} + \varphi_{Al2O3} \cdot k_{Al2o3}) - 2\varnothing_{hnf} \cdot k_{bf}\right)}{\frac{(\varphi_{Cuo} \cdot k_{cuo} + \varphi_{Al2O3} \cdot k_{Al2o3})}{\varnothing_{hnf}} + 2k_{bf} - 2(\varphi_{Cuo} \cdot k_{cuo} + \varphi_{Al2O3} \cdot k_{Al2o3}) + \varnothing_{hnf} \cdot k_{bf}} \tag{6}$$

4. Rayleigh and Nusselt Numbers and Validation

The Rayleigh and Nusselt numbers of the hybrid nanofluids could be computed using the heating power, the observed temperatures of the left and right walls, and the transport properties as below:

$$Q_h = V \times I \tag{7}$$

The heat transfer on the cold side of the heat exchanger is estimated by:

$$Q_c = \dot{m} \cdot Cp \times (T_{co} - T_{ci}) \tag{8}$$

where T_{ci} and T_{co} are the inlet and outlet temperatures on the cold wall, respectively.

The heat transfer coefficient could be calculated as:

$$h = \frac{Q}{A(T_h - T_c)} \tag{9}$$

The Rayleigh number could be calculated as:

$$Ra = \frac{g\beta\delta^2 Cp(T_h - Tc)L^3}{\mu K} \tag{10}$$

The Nusselt number could be calculated using the correlation equation as a function of the *Ra* and *Pr* provided by Berkovesky and Polevikov [39], as given below:

$$Nu = 0.18\left(\frac{Pr}{0.2+Pr}Ra\right)^{0.29} \qquad 1 < \frac{H}{L}\ 2 \qquad and \qquad \frac{Ra \times Pr}{0.2+Pr}\ 10^{3} \tag{11}$$

Catton [40] also gives a correlation for *Nu* given in Equation (12):

$$Nu = 0.22\left(\frac{Pr}{0.2+Pr}Ra\right)^{0.28} \qquad \left(\frac{H}{L}\right)^{\frac{-1}{4}} \qquad 1 < \frac{H}{L} < 2, \quad and \quad Ra < 10^{10} \tag{12}$$

This is inferred from experimental findings compared to previously documented correlations of water's natural convection in an enclosure, as illustrated in the graph below, Figure 4.

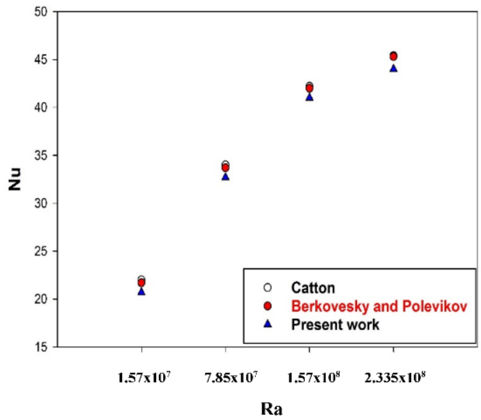

Figure 4. Validation of the experimental setup using Nu as a function of Ra in comparison to the existence of correlations.

The experimental results for the water-filled cavity showed good agreement with the correlation of Berkovesky and Polevikov [39] and Catton [40].

5. Results

This work examined the natural convection of a (50%CuO–50%Al_2O_3)/water hybrid nanofluid in a rectangular cavity with PCM connected to its vertical hot wall. Various parameters' effects were investigated, including the concentration of nanoparticles ($0.03 \leq \varphi \leq 0.05$), cavity inclination angle ($0° \leq \theta \leq 45°$), the temperature difference between the cold and hot walls ($10 \leq \Delta T \leq 20$) °C, and times at ($15 \leq$ time ≤ 60) min.

The experimental results are presented in complete thermal camera temperature distribution results and thermocouple data collected along the midline of the cavity. Figures 5 and 6 show the temperature distribution with time using full PCM ϕ = 0.03%, ΔT = 10°, 15°, and 20 °C. When the hot wall temperature was 35 °C (ΔT = 10 °C), PCM solubility was not recorded even on reaching a steady state. This happened due to the high latent heat of paraffin wax. A constant decline rate for the temperature of the PCM at the top cavity had a greater temperature than at the bottom, and the difference approached 3 °C due to free convection currents in the hybrid nanofluid cavity caused by the buoyant force. In a hybrid nanofluid cavity, the heat transfers from the lift wall to the cold wall. At a time of 15 min, the high temperature could be seen near the top left corner due to the buoyant force. After a period of time (30 min), the heat transferred along the vertical wall, and the fluid flow moved faster, which meant that heat transferred quicker, and all the cavity temperatures rose. After more time, at 60 min, most of the heat transferred to the cold side, and the heat was kept at a lower level. A consistent decline rate for the hot wall temperature was recorded at 11%. The same behavior could be seen after raising the temperature of the hot wall to 40 °C(ΔT = 15 °C). It can be seen that the heat transmission through conduction was dominating, and the rate of decrease in the hot wall temperature was 18%.

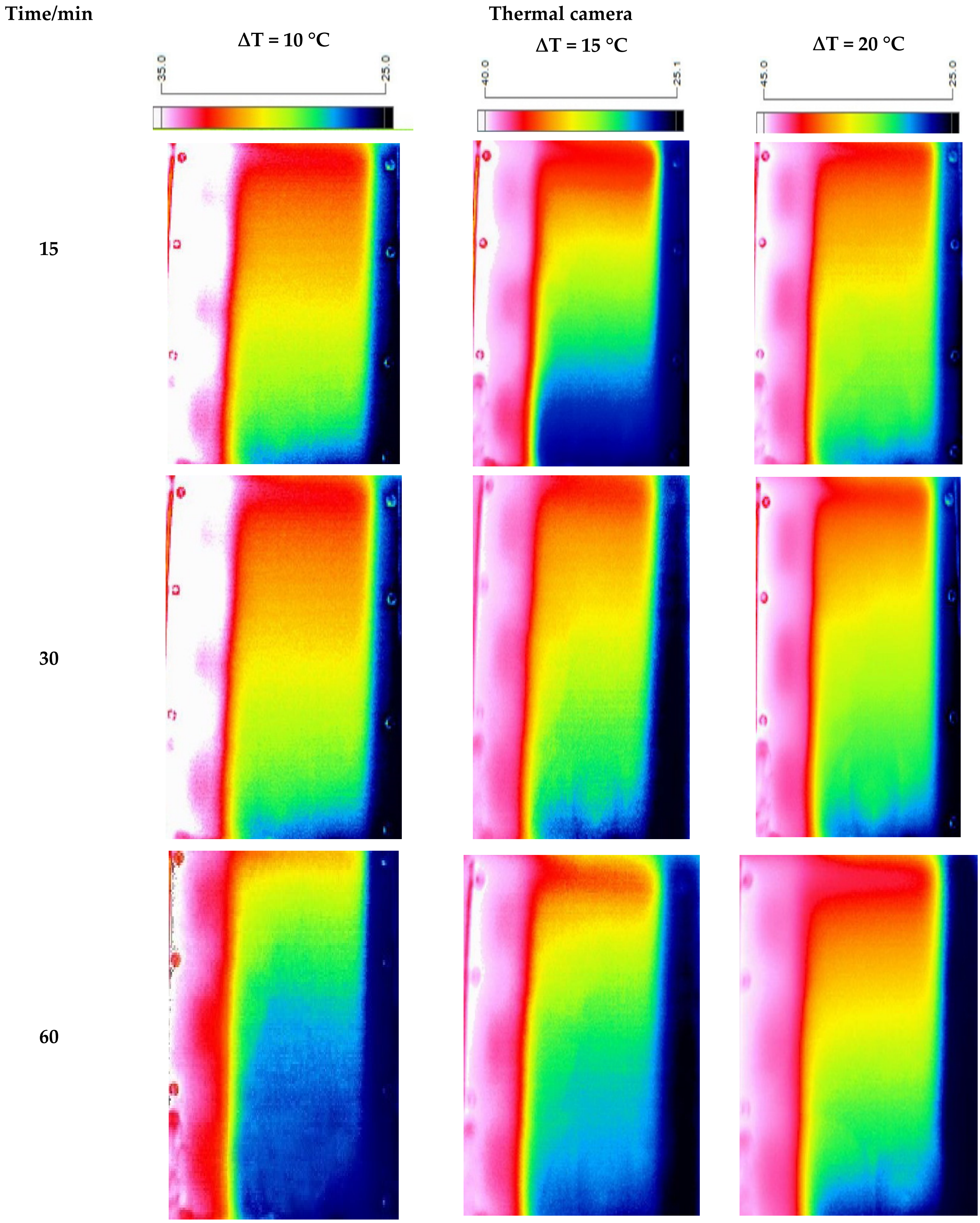

Figure 5. Temperature distribution in the enclosures at various times for the PCM and hybrid nanofluid at $\varphi = 0.03$, $\theta = 0°$, ΔT = 10, 15 and 20 °C.

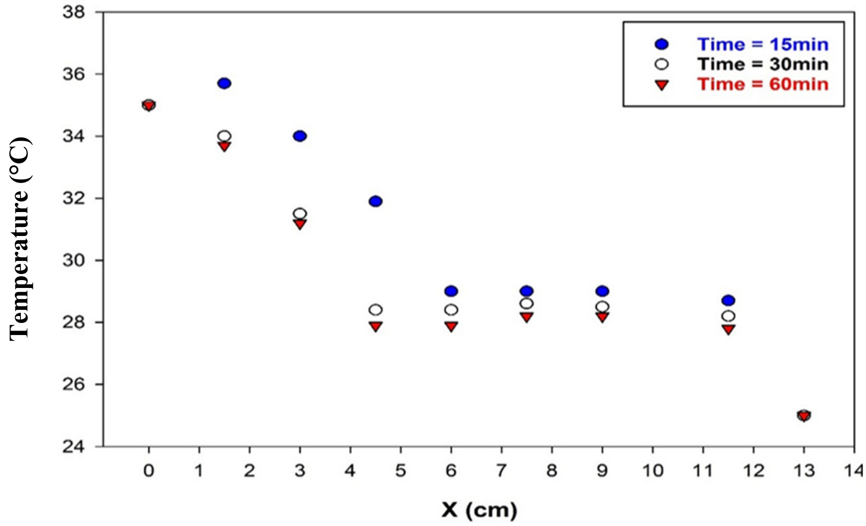

(**a**)

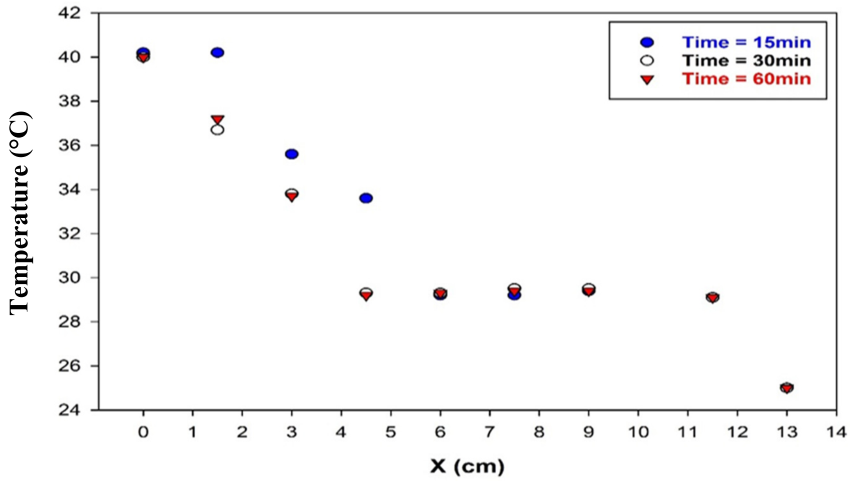

(**b**)

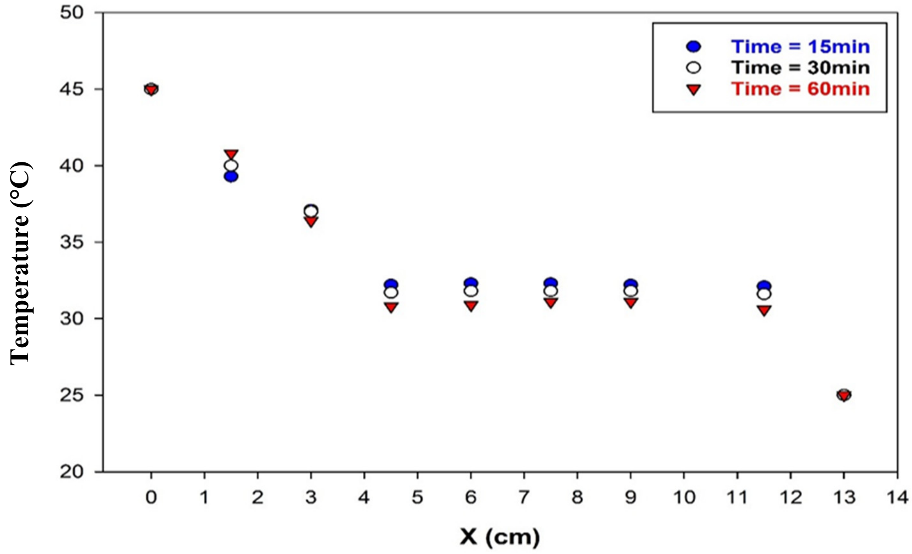

(**c**)

Figure 6. Temperature profiles at midline of the enclosures at various times for the PCM and hybrid nanofluid at $\varphi = 0.03$, $\theta = 0^{\circ}$: (**a**) at $\Delta T = 10\ ^{\circ}C$, (**b**) at $\Delta T = 15\ ^{\circ}C$, (**c**) at $\Delta T = 20\ ^{\circ}C$.

When the hot wall temperature rose to 45 °C (ΔT = 20 °C), the paraffin wax became relatively liquid, especially near the top of the cavity. The heat transfer was dominated by free convection, with the maximum temperature on the upper left side of the PCM cavity and the lowest temperature on the bottom right side of the other cavity filled with a hybrid nanofluid. In this case, the decreased hot wall temperature rate was 21%. In general, the melting rate of paraffin wax increased as the hot wall temperature rose (over 38 °C), but it did not reach the complete melting stage even when the hot wall temperature was higher than the melting point of paraffin wax. This was due to the impact of the hybrid nanofluid, which accelerated heat transfer via free convection (heat removal), allowing the wall adherent to the right wall of the PCM cavity to remain cool. In addition, as time passed the effect of heat transfer via natural convection due to the buoyant force and the related vortices could be seen in the hybrid nanofluid cavity, as shown in Figure 6. When the amount of removed heat increased, the temperature inside the cavity decreased. This was demonstrated by the enhanced heat transport rate and temperature reduction of the PCM, which sped up the cooling process of the heated wall.

Figures 7 and 8 show the temperature distribution with time when the hybrid nanofluid was at ϕ = 0.03%, θ = 30°, ΔT = 10, 15, and 20 °C. When the hot wall temperature was 35 °C (ΔT = 10), the heat transmission by conduction was dominant due to the paraffin wax not remaining in its solid condition. The temperature reduction rate in the paraffin wax cavity was 10.9%. When the hot wall temperature was 40 °C (ΔT = 15 C), a reduced rate of 16% was recorded. When the hot wall temperature reached 45 °C, the paraffin wax began to melt, and the rate of temperature decrease was 20.4%.

The same behavior could be seen when θ = 45°, as shown in Figures 9 and 10. The results show that the reduction rates were 13%, 18.25%, and 21.5% when ΔT equaled 10, 15, and 20 °C, respectively. Figures 11–13 show the temperature distribution along the midline of the cavities with time using PCM when the hybrid nanofluid was at ϕ = 0.05%, θ = 0°, 30°, and 45°, ΔT = 10, 15, and 20 °C. The same behavior can be seen when the inclination angle changed from 0 to 45°, and the temperature increased by increasing the hybrid nanofluid volume fraction. The maximum heat reduction was 22.2% when θ = 30°.

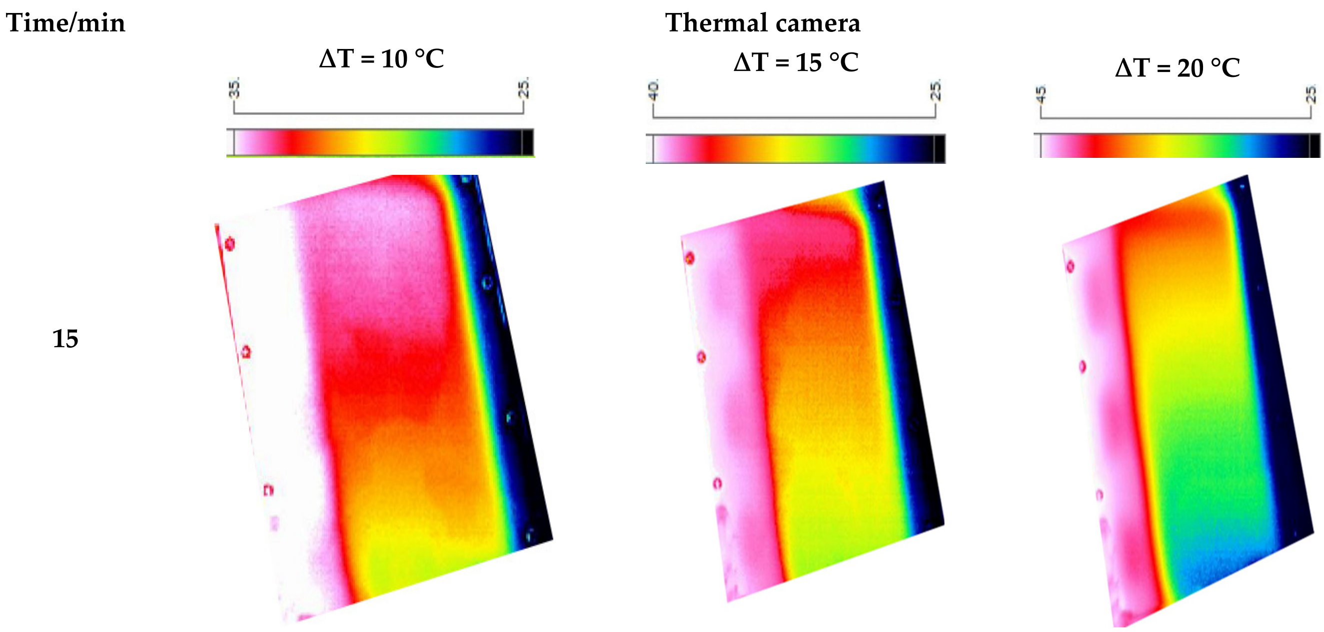

Figure 7. *Cont.*

30

60

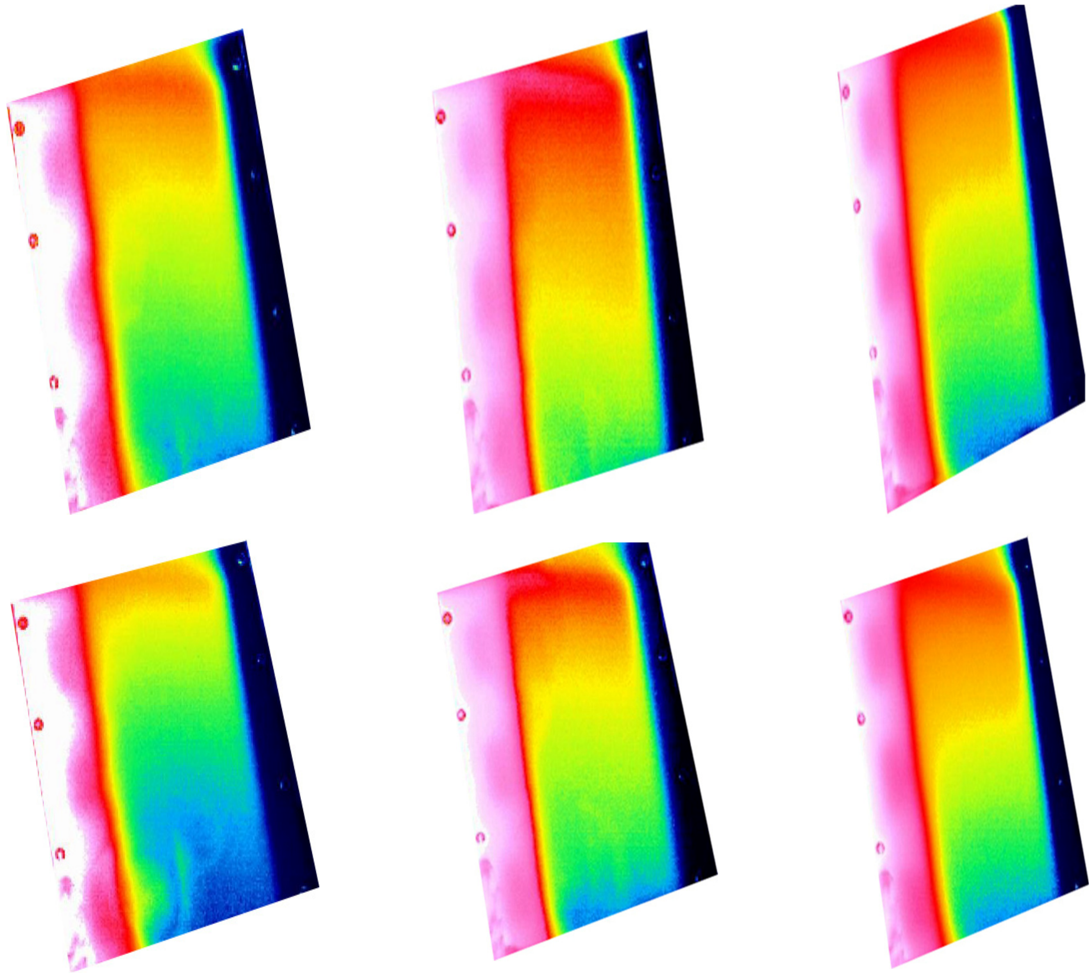

Figure 7. Temperature distribution in the enclosure at various time for PCM and (CuO-Al_2O_3/water), $\Phi = 0.03$, $\theta = 30°$, $\Delta T = 10$, 15, and 20 °C.

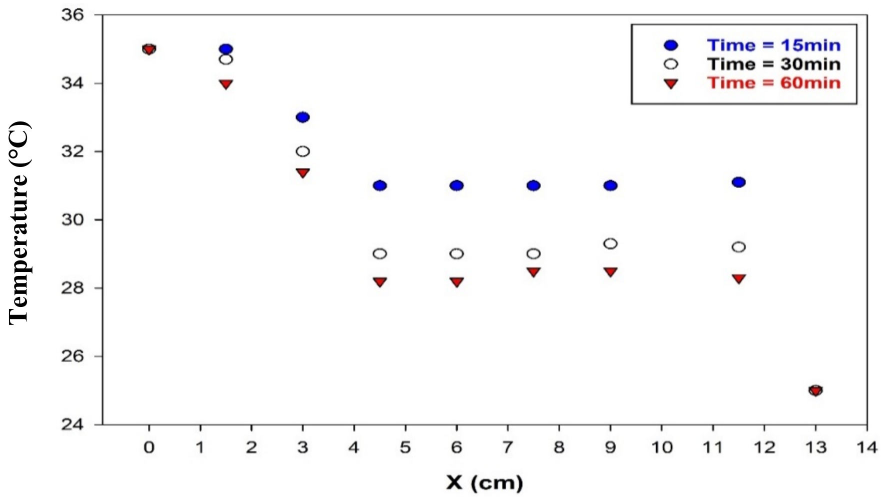

(**a**)

Figure 8. *Cont.*

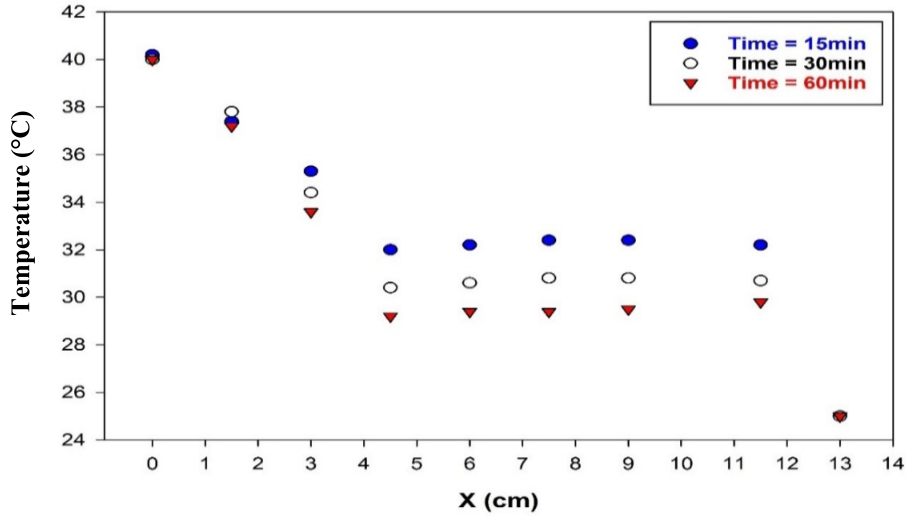

(**b**)

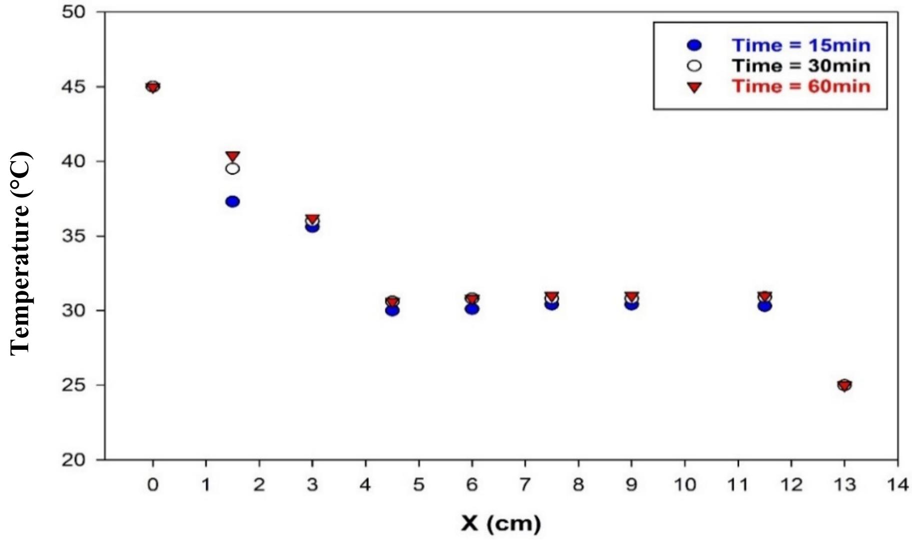

(**c**)

Figure 8. Temperature profiles at midline of the enclosures at various time for the PCM and hybrid nanofluid at $\varphi = 0.03$, $\theta = 30°$: (**a**) at ΔT = 10 °C, (**b**) at ΔT = 15 °C, (**c**) at ΔT = 20 °C.

The Nusselt number was calculated using the correlation equation on the left wall of the hybrid nanofluid cavity. Due to using a PCM, the left-side hot temperature was not constant, whereas the cold wall temperature was maintained at 25 °C. The Nusselt number could determine and quantify the amount of heat transfer by free convection inside the hybrid nanofluid cavity and the effect of phase change materials on the hot wall during the heat transmission process. Nusselt numbers were performed at various hot wall temperatures (T = 35, 40, and 45 °C), concentrations, and cavity inclination angles.

Figure 14 displays the average Nusselt number for various values of the temperature difference and various cavity inclination angles. It was found that by increasing the concentration of hybrid nanomaterial, the Nusselt number increased for different values of cavity inclination angle. The reason for this was increase in the thermal conductivity of a hybrid nanofluid, which accelerates the flow of convection between opposite vertical cavity walls. In addition, the Nusselt number increased as the temperature difference increased due to the cavity containing the hybrid nanofluids' increased capacity for heat transfer due to temperature difference. It was found that irrespective of the base fluid composition, the heat enhancement was highest at the inclination angle θ = 30°.

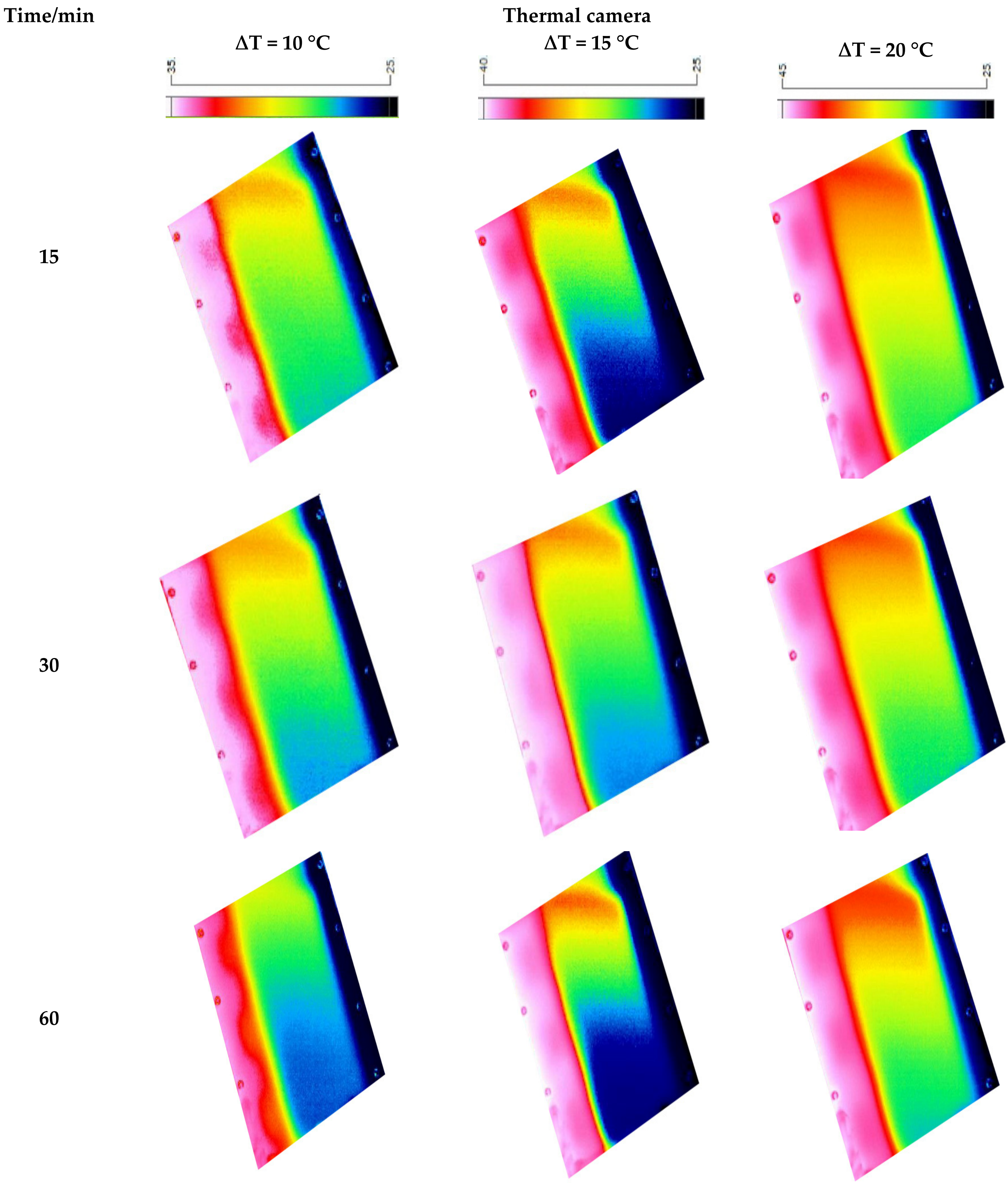

Figure 9. Temperature distribution in the enclosure at various times for PCM and (CuO-Al_2O_3/water), $\Phi = 0.03$, $\theta = 45°$, $\Delta T = 10$, 15, and 20 °C.

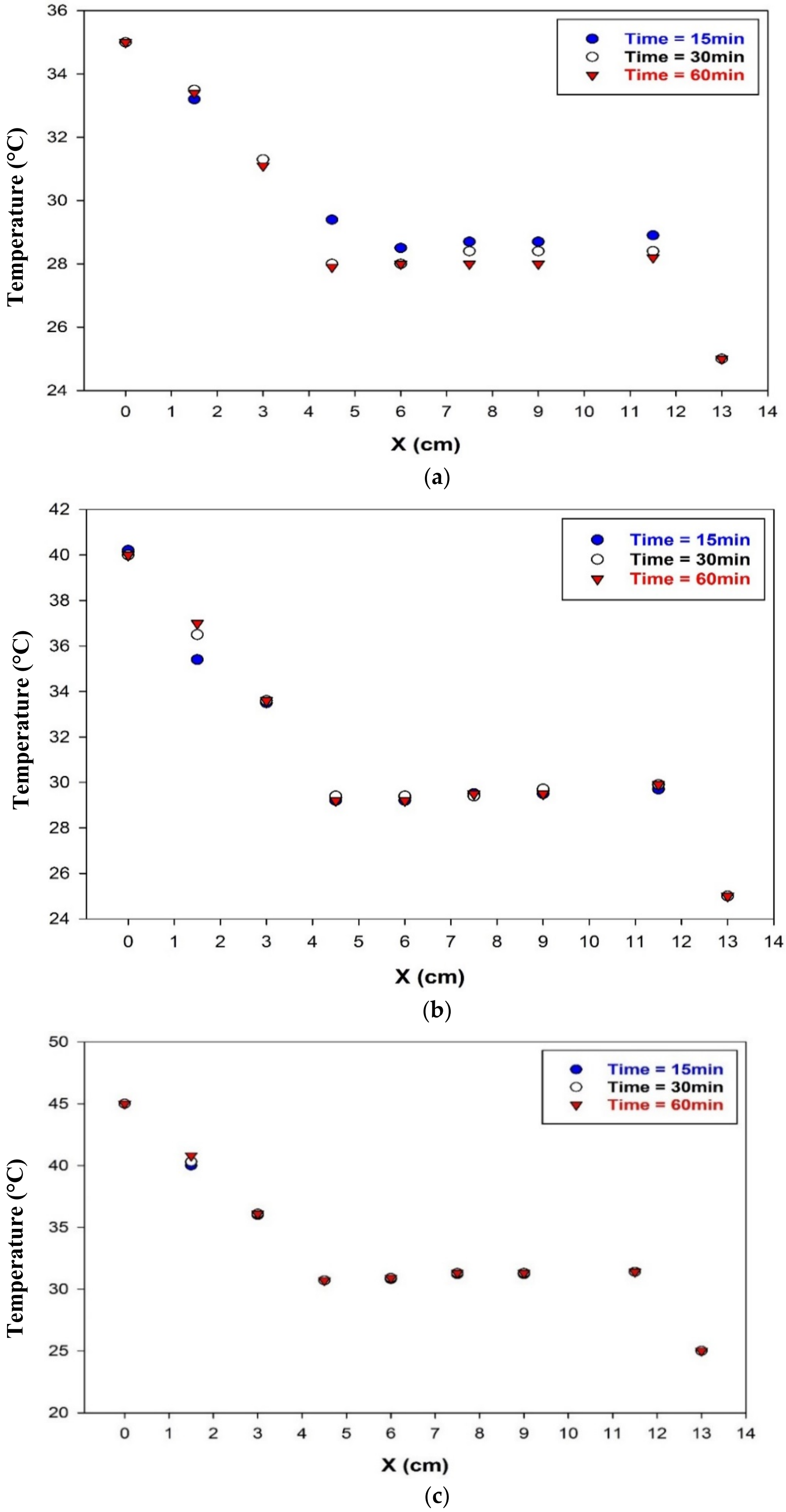

Figure 10. Temperature profiles at the midline of the enclosures at various times for the PCM and hybrid nanofluid at $\varphi = 0.03$, $\theta = 45°$: (**a**) at $\Delta T = 10$ °C, (**b**) at $\Delta T = 15$ °C, (**c**) at $\Delta T = 20$ °C.

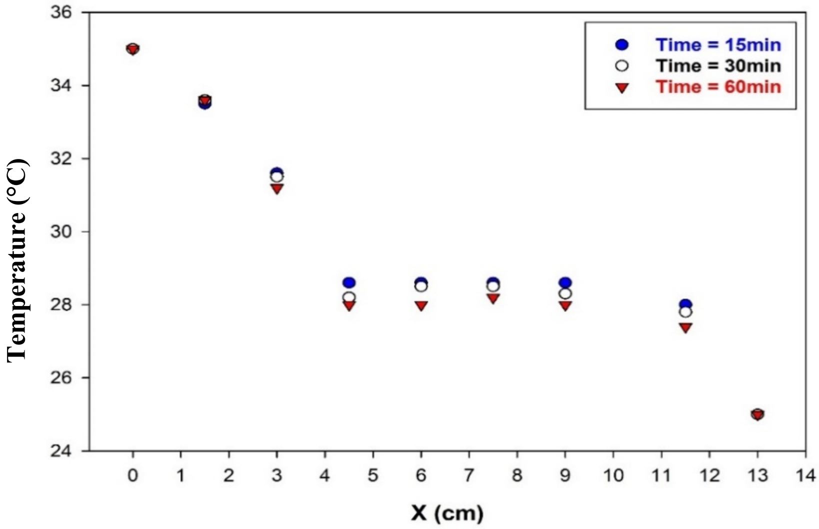

(**a**)

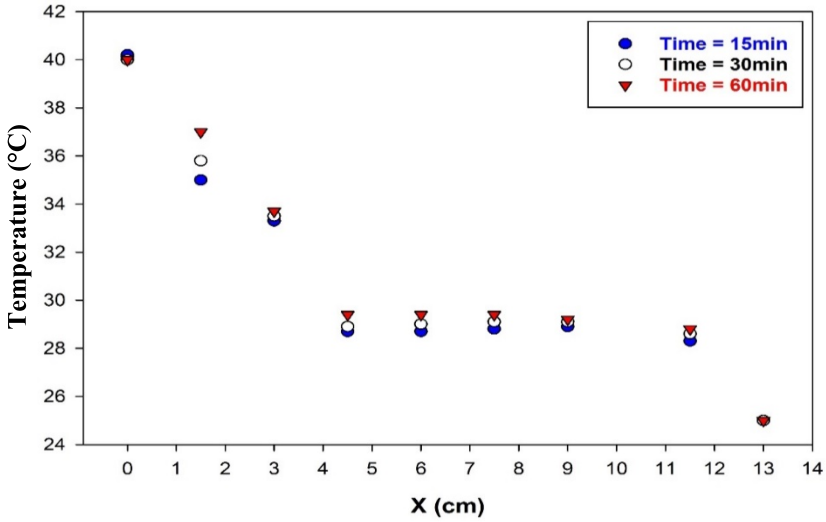

(**b**)

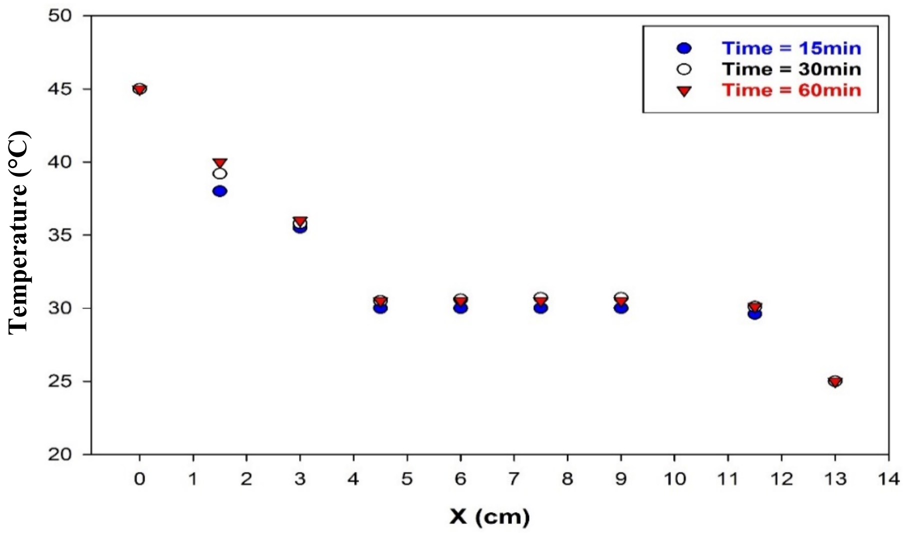

(**c**)

Figure 11. Temperature profiles at the midline of the enclosures at various times for the PCM and hybrid nanofluid at $\varphi = 0.05$, $\theta = 0°$: (**a**) at $\Delta T = 10$ °C, (**b**) at $\Delta T = 15$ °C, (**c**) at $\Delta T = 20$ °C.

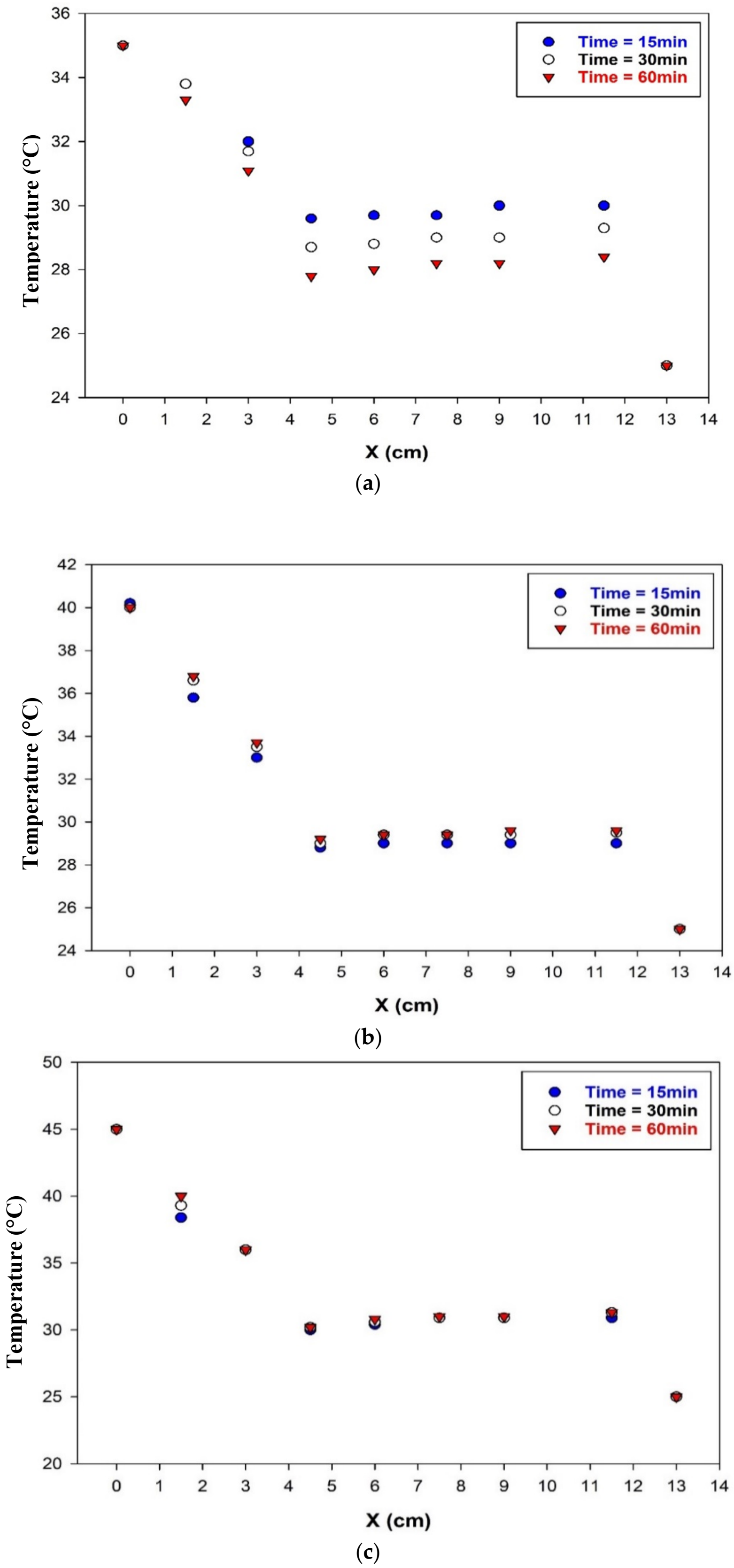

Figure 12. Temperature profiles at the midline of the enclosures at various times for the PCM and hybrid nanofluid at $\varphi = 0.05$, $\theta = 30°$: (**a**) at $\Delta T = 10$ °C, (**b**) at $\Delta T = 15$ °C, (**c**) at $\Delta T = 20$ °C.

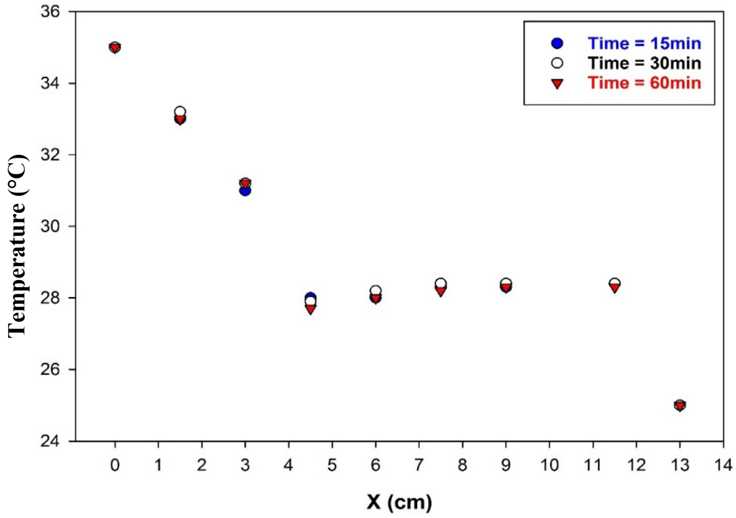

(**a**)

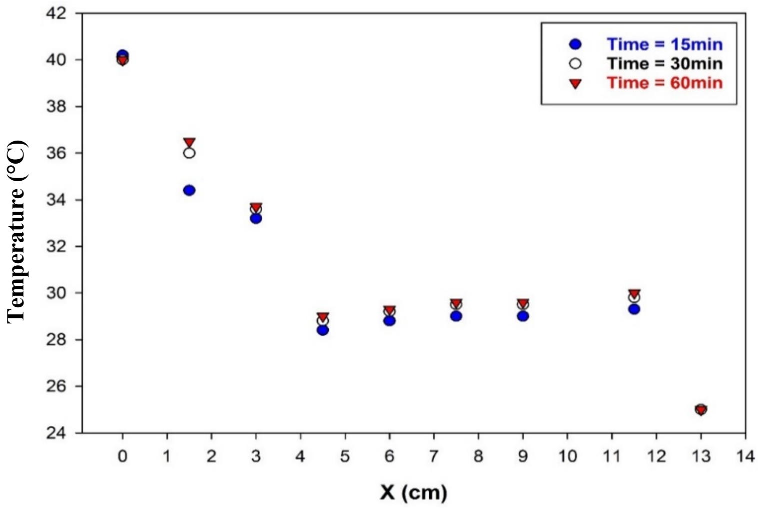

(**b**)

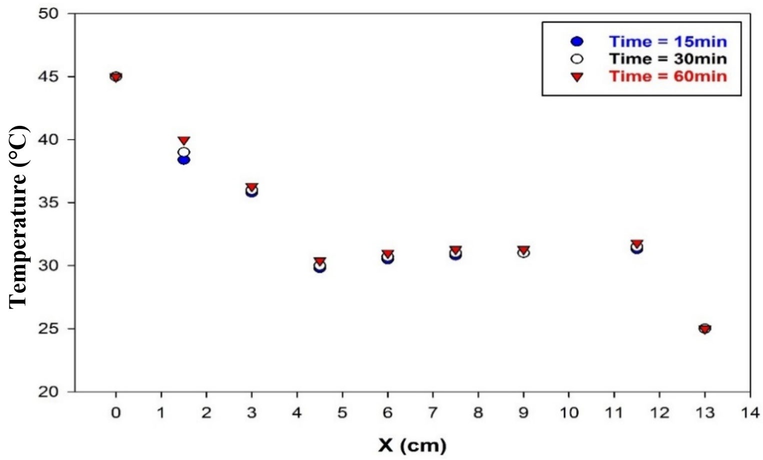

(**c**)

Figure 13. Temperature profiles at the midline of the enclosures at various times for the PCM and hybrid nanofluid at $\varphi = 0.05$, $\theta = 45°$: (**a**) at $\Delta T = 10$ °C, (**b**) at $\Delta T = 15$ °C, (**c**) at $\Delta T = 20$ °C.

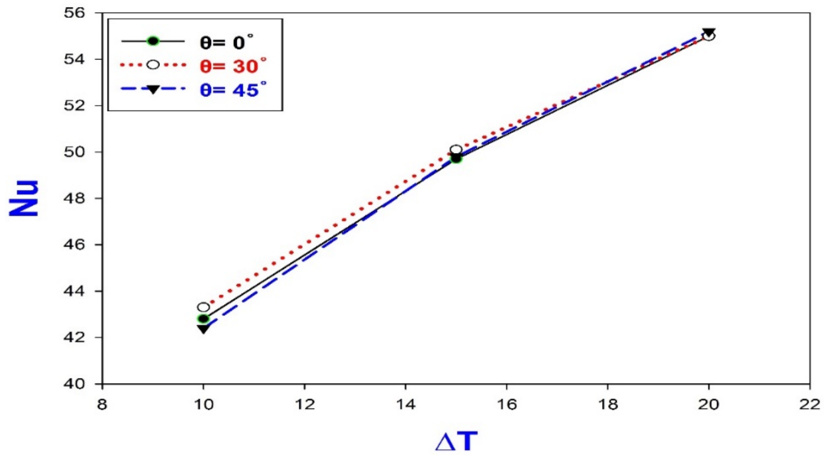

(**a**)

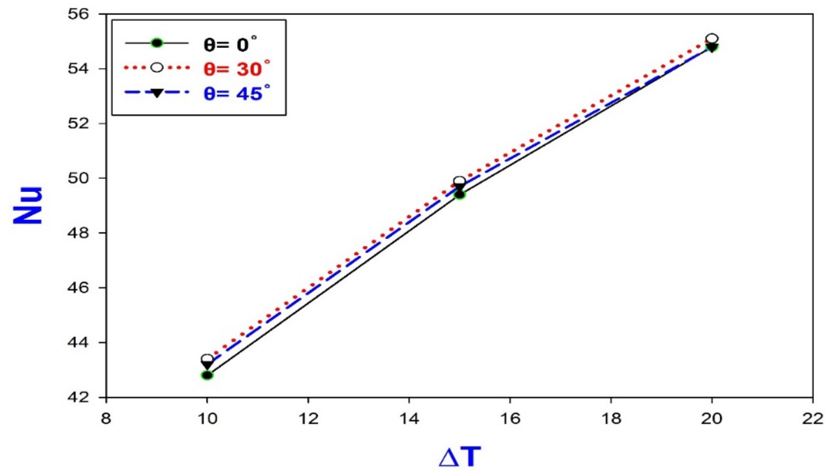

(**b**)

Figure 14. Effect of the average Nusselt number along the left wall with temperature difference at (**a**) φ = 0.03% and (**b**) φ = 0.05%.

6. Conclusions

An experimental study of natural convective heat transfer in a rectangular cavity filled with a (50%CuO–50%Al_2O_3)/water hybrid nanofluid with phase change material connected to its vertical hot wall was investigated in this study, and the impacts of several parameters were examined, including: nanoparticle concentration φ = 0.03% and 0.05%, inclination angle of the cavity θ = 0°, 30°, and 45°, temperature difference between the cold and hot walls ΔT = 10 °C, 15 °C, and 20 °C, and time effects at 15, 30, and 60 min.

The following are some significant conclusions that may be drawn from the experimental results:

1. In general, temperatures were observed to be more widely distributed in the upper half of the cavity due to the effects of buoyant force and different densities on natural convection.
2. When the concentration of hybrid nanofluid was increased, the thermal conductivity increased; therefore, the reduction rate of heat transfer increased due to the high thermal conductivity of the hybrid nanomaterial.
3. The effect of the cavity inclination angle on heat transfer was pronounced, with θ = 30° being the optimal angle for temperature reduction, where its reduction rate reached the highest value (22.2%) compared to θ = 0°.

4. The temperature differential between hot and cold walls affected the reduction rate where proportionality was established between them, with the greatest value occurring when $\Delta T = 20\ ^\circ C$, and 22% was reached.
5. The value of the Nusselt number increased by increasing the temperature difference, which happened due to the increase in the buoyant force in the hybrid nanofluid cavity.
6. Increase in the Nusselt number means an increase in the natural convection heat transmission rate in the nanofluid cavity, but at the same time indicates that a large amount of heat crossed through the middle wall due to the lack of paraffin wax, which was responsible for lowering the temperature.
7. Adding paraffin wax along the hot wall was the optimal method for lowering the temperature of the wall by absorbing the high heat and decreasing the transient heat of the nanofluid cavity.
8. The Nusselt number increased with increasing nanomaterial concentration, which was caused by greater heat exchange between the paraffin wax and the hybrid nanofluid. Heat transfer via natural convection increased as thermal conductivity rose, as we have previously shown by increasing the hybrid nanofluid concentration.

Future work could consider new types of nanomaterials to study the effects of adding different types of nanofluids. Some new complex geometries can be also considered, which need to choose a suitable position for the PCM. Furthermore, it is worthwhile to use different types of PCM to study their effects on heat transfer.

Author Contributions: Conceptualization, K.A.-F. and M.A.-M.; methodology, K.A.-F.; experimental, K.A.-F. and M.A.-M.; validation, M.A.-M.; investigation, I.E.S., resources, M.A.-M.; writing—original draft preparation, M.A.-M. and K.A.-F.; writing—review and editing, K.A.-F. and I.E.S.; supervision, K.A.-F.; project administration, K.A.-F.; funding acquisition, I.E.S. All authors have read and agreed to the published version of the manuscript.

Funding: This research received no external funding.

Data Availability Statement: Not applicable.

Conflicts of Interest: The authors declare no conflict of interest.

Nomenclature

A	Area
Cp	Specific heat, $J \cdot kg^{-1} \cdot K^{-1}$
g	The acceleration of gravity, $m \cdot s^{-2}$
h	Heat transfer coefficient
I	Current (ampere)
K	Thermal conductivity, $W \cdot m^{-1} \cdot K^{-1}$
$\dot{m}$	Mass flow rate of the fluid
Nu	Nusselt number
P	Non-dimensional pressure
PCM	Phase change material
Pr	Prandtl number
Q	Heat transfer
Ra	Rayleigh number
T_c	Cold temperature, K
T_h	Hot temperature, K
V	Voltage (volts)
Greek symbols	
θ	Inclination angle of the cavity
μ	Dynamic viscosity, $kg \cdot m^{-1} \cdot s^{-1}$
α	Thermal diffusivity, $m^2 \cdot s^{-1}$
β	Thermal expansion coefficient, K^{-1}
Φ	Volume concentration of the nanofluid

References

1. Sadeghi, M.S.; Anadalibkhah, N.; Ghasemiasl, R.; Armaghani, T.; Dogonchi, A.S.; Chamkha, A.J.; Ali, H.; Asadi, A. On the natural convection of nanofluids in diverse shapes of enclosures: An exhaustive review. *J. Therm. Anal.* **2020**, *147*, 1–22. [CrossRef]
2. Aljabair, S.; Mohammed, A.A.; Alesbe, I. Natural convection heat transfer in corrugated annuli with H2O-Al2O3 nanofluid. *Heliyon* **2020**, *6*, e05568. [CrossRef] [PubMed]
3. Abdulsahib, A.D.; Al-Farhany, K. Review of the Effects of Stationary/Rotating Cylinder in a Cavity on the Convection Heat Transfer in Porous Media with/without Nanofluid. *Math. Model. Eng. Probl.* **2021**, *8*, 356–364. [CrossRef]
4. Al-Chlaihawi, K.K.; Alaydamee, H.H.; Faisal, A.E.; Al-Farhany, K.; Alomari, M.A. Newtonian and non-Newtonian nanofluids with entropy generation in conjugate natural convection of hybrid nanofluid-porous enclosures: A review. *Heat Transf.* **2021**, *51*, 1725–1745. [CrossRef]
5. Abdulsahib, A.D.; Al-Farhany, K. Numerical investigation of the nanofluid mixed convection on two layers enclosure with rotating cylinder: High Darcy number effects. In *IOP Conference Series: Materials Science and Engineering*; IOP Publishing: Bristol, UK, 2020. [CrossRef]
6. Tayebi, T.; Öztop, H.F.; Chamkha, A.J. Natural convection and entropy production in hybrid nanofluid filled-annular elliptical cavity with internal heat generation or absorption. *Therm. Sci. Eng. Prog.* **2020**, *19*, 100605. [CrossRef]
7. Amine, B.M.; Redouane, F.; Mourad, L.; Jamshed, W.; Eid, M.R.; Al-Kouz, W. Magnetohydrodynamics Natural Convection of a Triangular Cavity Involving Ag-MgO/Water Hybrid Nanofluid and Provided with Rotating Circular Barrier and a Quarter Circular Porous Medium at its Right-Angled Corner. *Arab. J. Sci. Eng.* **2021**, *46*, 12573–12597. [CrossRef]
8. Revnic, C.; Groşan, T.; Sheremet, M.; Pop, I. Numerical simulation of MHD natural convection flow in a wavy cavity filled by a hybrid Cu-Al2O3-water nanofluid with discrete heating. *Appl. Math. Mech.* **2020**, *41*, 1345–1358. [CrossRef]
9. Chamkha, A.J.; Miroshnichenko, I.V.; Sheremet, M.A. Numerical Analysis of Unsteady Conjugate Natural Convection of Hybrid Water-Based Nanofluid in a Semicircular Cavity. *J. Therm. Sci. Eng. Appl.* **2017**, *9*, 041004. [CrossRef]
10. Wang, L.; Yang, X.; Huang, C.; Chai, Z.; Shi, B. Hybrid lattice Boltzmann-TVD simulation of natural convection of nanofluids in a partially heated square cavity using Buongiorno's model. *Appl. Therm. Eng.* **2018**, *146*, 318–327. [CrossRef]
11. Alomari, M.A.; Al-Farhany, K.; Hashem, A.L.; Al-Dawody, M.F.; Redouane, F.; Olayemi, O.A. Numerical Study of MHD Natural Convection in Trapezoidal Enclosure Filled With (50%MgO-50%Ag/Water) Hybrid Nanofluid: Heated Sinusoidal from Below. *Int. J. Heat Technol.* **2021**, *39*, 1271–1279. [CrossRef]
12. Redouane, F.; Jamshed, W.; Devi, S.S.U.; Amine, B.M.; Safdar, R.; Al-Farhany, K.; Eid, M.R.; Nisar, K.S.; Abdel-Aty, A.-H.; Yahia, I.S. Influence of entropy on Brinkman–Forchheimer model of MHD hybrid nanofluid flowing in enclosure containing rotating cylinder and undulating porous stratum. *Sci. Rep.* **2021**, *11*, 24316. [CrossRef]
13. Kheradmand, M.; Abdollahzadeh, M.; Azenha, M.; de Aguiar, J. Phase change materials as smart nanomaterials for thermal energy storage in buildings. *Intell. Nanomater.* **2016**, *2*, 247–293.
14. Hong, Y.; Ye, W.-B.; Du, J.; Huang, S.-M. Solid-liquid phase-change thermal storage and release behaviors in a rectangular cavity under the impacts of mushy region and low gravity. *Int. J. Heat Mass Transf.* **2019**, *130*, 1120–1132. [CrossRef]
15. Parsazadeh, M.; Malik, M.; Duan, X.; McDonald, A. Numerical study on melting of phase change material in an enclosure subject to Neumann boundary condition in the presence of Rayleigh-Bénard convection. *Int. J. Heat Mass Transf.* **2021**, *171*, 121103. [CrossRef]
16. Bouhal, T.; Fertahi, S.E.-D.; Limouri, O.; Agrouaz, Y.; Kousksou, T.; Zeraouli, Y.; Jamil, A. Numerical analysis of PCM melting filling a rectangular cavity with horizontal partial fins. In *MATEC Web of Conferences*; EDP Sciences: Les Ulis, France, 2020; p. 01011.
17. Chamkha, A.; Doostanidezfuli, A.; Izadpanahi, E.; Ghalambaz, M. Phase-change heat transfer of single/hybrid nanoparticles-enhanced phase-change materials over a heated horizontal cylinder confined in a square cavity. *Adv. Powder Technol.* **2017**, *28*, 385–397. [CrossRef]
18. Laouer, A.; Al-Farhany, K.; Al-Dawody, M.F.; Hashem, A.L. A numerical study of phase change material melting enhancement in a horizontal rectangular enclosure with vertical triple fins. *Int. Commun. Heat Mass Transf.* **2022**, *137*, 106223. [CrossRef]
19. Laouer, A.; Al-Farhany, K. Melting of nano-enhanced phase change material in a cavity heated sinusoidal from below: Numerical study using lattice Boltzmann method. *Heat Transf.* **2022**, *51*, 5952–5970. [CrossRef]
20. Koláček, M.; Charvátová, H.; Sehnálek, S. Experimental and Numerical Research of the Thermal Properties of a PCM Window Panel. *Sustainability* **2017**, *9*, 1222. [CrossRef]
21. Kułakowski, T.; Krempski-Smejda, M.; Heim, D. Heat Transfer with Phase Change in a Multilayer Construction: Simulation versus Experiment. *Energies* **2021**, *14*, 4390. [CrossRef]
22. Tomita, S.; Celik, H.; Mobedi, M. Thermal Analysis of Solid/Liquid Phase Change in a Cavity with One Wall at Periodic Temperature. *Energies* **2021**, *14*, 5957. [CrossRef]
23. Ye, R.; Fang, X.; Zhang, Z. Numerical Study on Energy-Saving Performance of a New Type of Phase Change Material Room. *Energies* **2021**, *14*, 3874. [CrossRef]
24. Abderrahmane, A.; Al-Khaleel, M.; Mourad, A.; Laidoudi, H.; Driss, Z.; Younis, O.; Guedri, K.; Marzouki, R. Natural Convection within Inversed T-Shaped Enclosure Filled by Nano-Enhanced Phase Change Material: Numerical Investigation. *Nanomaterials* **2022**, *12*, 2917. [CrossRef] [PubMed]

25. Abderrahmane, A.; Qasem, N.A.A.; Mourad, A.; Al-Khaleel, M.; Said, Z.; Guedri, K.; Younis, O.; Marzouki, R. Enhancing the Melting Process of Shell-and-Tube PCM Thermal Energy Storage Unit Using Modified Tube Design. *Nanomaterials* **2022**, *12*, 3078. [CrossRef] [PubMed]
26. Abderrahmane, A.; Younis, O.; Al-Khaleel, M.; Laidoudi, H.; Akkurt, N.; Guedri, K.; Marzouki, R. 2D MHD Mixed Convection in a Zigzag Trapezoidal Thermal Energy Storage System Using NEPCM. *Nanomaterials* **2022**, *12*, 3270. [CrossRef]
27. Shili, H.; Fahem, K.; Harmand, S.; Ben Jabrallah, S. Thermal control of electronic components using a liquid around the phase change material. *J. Therm. Anal.* **2020**, *140*, 1177–1189. [CrossRef]
28. Kean, T.H.; Sidik, N.A.C.; Kaur, J. Numerical investigation on melting of Phase Change Material (PCM) dispersed with various nanoparticles inside a square enclosure. In *IOP Conference Series: Materials Science and Engineering*; IOP Publishing: Bristol, UK, 2019; p. 012034.
29. Sivashankar, M.; Selvam, C.; Manikandan, S.; Harish, S. Performance improvement in concentrated photovoltaics using nano-enhanced phase change material with graphene nanoplatelets. *Energy* **2020**, *208*, 118408. [CrossRef]
30. Ebadi, S.; Tasnim, S.H.; Aliabadi, A.A.; Mahmud, S. Melting of nano-PCM inside a cylindrical thermal energy storage system: Numerical study with experimental verification. *Energy Convers. Manag.* **2018**, *166*, 241–259. [CrossRef]
31. Abdelrazik, A.; Al-Sulaiman, F.; Saidur, R. Numerical investigation of the effects of the nano-enhanced phase change materials on the thermal and electrical performance of hybrid PV/thermal systems. *Energy Convers. Manag.* **2020**, *205*, 112449. [CrossRef]
32. Nada, S.; El-Nagar, D.; Hussein, H. Improving the thermal regulation and efficiency enhancement of PCM-Integrated PV modules using nano particles. *Energy Convers. Manag.* **2018**, *166*, 735–743. [CrossRef]
33. Chavan, S.; Perumal, D.A.; Gumtapure, V. Numerical studies for charging and discharging characteristics of composite phase change material in a deep and shallow rectangular enclosure. In *IOP Conference Series: Materials Science and Engineering*; IOP Publishing: Bristol, UK, 2018; p. 012059. [CrossRef]
34. Akeiber, H.; Nejat, P.; Majid, M.Z.A.; Wahid, M.A.; Jomehzadeh, F.; Famileh, I.Z.; Calautit, J.K.; Hughes, B.R.; Zaki, S.A. A review on phase change material (PCM) for sustainable passive cooling in building envelopes. *Renew. Sustain. Energy Rev.* **2016**, *60*, 1470–1497. [CrossRef]
35. Dukhan, W.A.; Dhaidan, N.S.; Al-Hattab, T.A. Experimental investigation of the horizontal double pipe heat exchanger utilized phase change material. In *IOP Conference Series: Materials Science and Engineering*; IOP Publishing: Bristol, UK, 2020; p. 012148.
36. Hussain, S.H.; Rahomey, M.S. Comparison of Natural Convection Around a Circular Cylinder With Different Geometries of Cylinders Inside a Square Enclosure Filled With Ag-Nanofluid Superposed Porous-Nanofluid Layers. *J. Heat Transf.* **2019**, *141*, 022501. [CrossRef]
37. Al-Srayyih, B.M.; Gao, S.; Hussain, S.H. Effects of linearly heated left wall on natural convection within a superposed cavity filled with composite nanofluid-porous layers. *Adv. Powder Technol.* **2019**, *30*, 55–72. [CrossRef]
38. Mansour, M.; Siddiqa, S.; Gorla, R.S.R.; Rashad, A. Effects of heat source and sink on entropy generation and MHD natural convection of Al 2 O 3 -Cu/water hybrid nanofluid filled with square porous cavity. *Therm. Sci. Eng. Prog.* **2018**, *6*, 57–71. [CrossRef]
39. Berkovsky, B.; Polevikov, V. *Numerical Study of Problems on High-Intensive Free Convection*; Hemisphere Publishing: Minsk, Russia, 1977.
40. Catton, I. Natural convection in enclosures. In *International Heat Transfer Conference Digital Library*; Begel House Inc.: Danbury, CT, USA, 1978.